

Supplementary information Resolving DNA at Efficiencies of More than A Million Plates per Meter Using Bare Narrow Open Capillary without Sieving Matrix

Zaifang Zhu,^a Lei Liu,^b Wei Wang,^a Joann J. Lu,^a Xiayan Wang,^{b*} and Shaorong Liu^{a*}

Received (in XXX, XXX) Xth XXXXXXXXXX 20XX, Accepted Xth XXXXXXXXXX 20XX

DOI: 10.1039/b000000x

Experimental

Reagents and materials. NoLimitsTM DNA fragments (75 bp, 1.5 kbp, 5.0 kbp, 20.0 kbp) were obtained from Fermentas Life Sciences Inc. (Glen Burnie, MD). YOYO-1 was purchased from Molecular Probes (Eugene, OR). Fluorescein, tris(hydroxymethyl)aminomethane (Tris), ethylenediaminetetraacetic acid (EDTA), sodium hydroxide, and concentrated hydrochloric acid were products of Fisher Scientific (Fisher, PA). All solutions were prepared using DDI water from a NANO pure infinity ultrapure water system (Barnstead, Newton, WA), and filtered through a 0.22- μm filter (VWR, TX) and vacuum-degassed before use. Capillaries were purchased from Polymicro Technologies (Phoenix, AZ).

Preparation of Standard Samples. 50 ng/ μL stock solutions of individual DNA fragments were prepared by mixing the DNA with YOYO-1 at a dye-to-base-pair ratio of 1:10 in 10 mM TE buffer, and 1 mM fluorescein stock solution was obtained by dissolving the appreciate amount in 10 mM TE buffer. Samples were prepared by diluting the corresponding stock solutions with DDI water as required. All standard solutions were stored at 4 °C.

Preparation of chip injector. The procedure of fabricating round channels on a chip was described previously.^{S1} Briefly, a photomask with an image-symmetric pattern (containing several crosses) was utilized to yield semicircular cross grooves on two wafers. The radius of the semicircular grooves was ca. 190 μm . The two wafers were then face-to-face aligned and thermally bonded. Round-channel crosses were produced by dicing the above chip. Fig. S1 presents an image of chip injector using such a cross.

Laser-induced fluorescence (LIF) detector. Fig. S2 presents a schematic diagram of the LIF detector. Briefly, a 488-nm beam from an argon ion laser (Laserphysics, Salt Lake City, UT, USA) was reflected by a dichroic mirror (Q505LP, Chroma Technology, Rockingham, VT, USA) and focused onto the narrow capillary through an objective lens (206 and 0.5 NA, Rolyn Optics, Covina, CA, USA). A detection window was made at ~ 5 cm from the outlet end of the narrow capillary by removing the polyimide coating using a torch. The capillary was affixed to a capillary holder which was attached to an x–y–z translation stage to align the detection window with the optical system to maximize the fluorescent output. Fluorescence from the capillary was collimated by the same objective lens, and collected by a

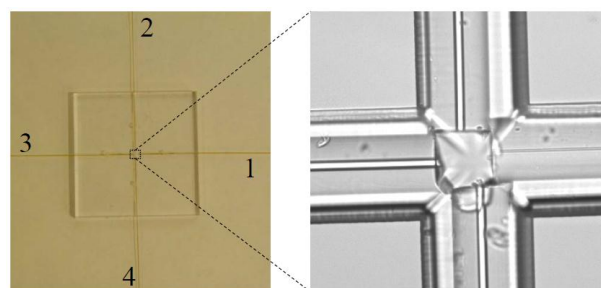


Fig. S1 Image of microfabricated chip injector with capillaries already attached to it. Inset – zoom-in view of the crossing area of the chip injector.

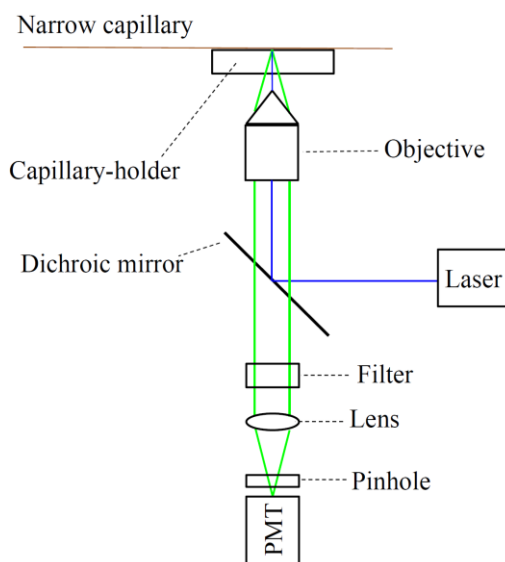


Fig. S2 LIF Detector

photosensor module (H5784-01, Hamamatsu, Japan) after passing through the dichroic mirror, an interference band-pass filter (532 nm), and a 2-mm pinhole. The output of the photosensor module was measured using a NI multifunctional card DAQCard-6062E (National Instruments, Austin, TX, USA). The data were acquired and treated with program written in-laboratory with Labview (National Instruments).

Alignment of detection window with LIF detector. Referring to

Fig. S2, after 20 μ M fluorescein solution was introduced to the narrow capillary, the position of the detection window was adjusted via the translation stage, while the fluorescence signal was monitored. Once the maximum signal output was reached, the x, y and z positions of the translation stage were locked, and the detection window was considered to be aligned with the LIF detector. The fluorescein solution should be thoroughly rinsed before performing BaNC-HDC separations.

Linear coefficients: As HETP values were linearly fitted with u , a set of linear regression coefficients (R^2) were generated. They were 0.913, 0.980, 0.981, 0.851, 0.983, 0.917, 0.962, 0.998, 0.974, 0.973, 0.975, 0.992, 0.997, 0.993, and 0.900 for 0.075, 0.1, 0.2, 0.3, 0.4, 0.5, 0.7, 1, 1.5, 2, 3, 4, 5, 7, 10, and 20 kbp DNA fragments.

Effect of DNA size on number of theoretical plates: In general, the number of theoretical plates decreased with the increase of the DNA size.

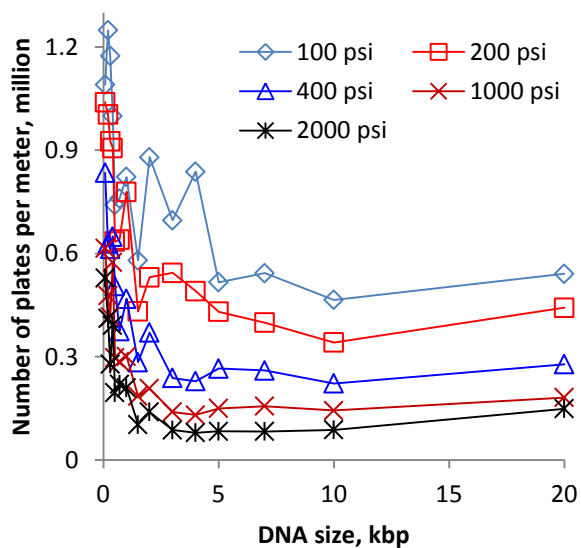


Fig. S3 Relationship between number of plates and DNA size

20

Notes and references

S1 S. Liu, *Electrophoresis* 2003, **24**, 3755.